ISSN: 2634-9221
European Journal of Applied Sciences; Vol. 14 No. 03 (2026) (624-634)
https://doi.org/10.14738/ejas.1403.11929

Scaling Properties of the Δγ Correlator: Constraints on Background and CME-Sensitive Charge Separation in Heavy-Ion Collisions

Roy A. Lacey* & Niseem Magdy

1. Depts. of Chemistry and Physics, Stony Brook University, Stony Brook, New York 11794, USA
2. Dept. of Physics, Texas Southern University, Houston, TX 77004, USA

Abstract: The scaling properties of the Δγ correlator, guided by calculations from the Anomalous Viscous Fluid Dynamics (AVFD) model, are used to investigate charge separation in p+Au, d+Au, Ru+Ru, Zr+Zr, and Au+Au collisions at $\sqrt{s_{NN}}$=200 GeV, and in p+Pb and Pb+Pb collisions at $\sqrt{s_{NN}}$=5.02 and 2.76 TeV. The ratio $\Delta\gamma/v_2$, where v_2 is the elliptic-flow coefficient, exhibits a common approximate $1/N_{ch}$ scaling behavior for p+Au, d+Au, p+Pb, and Pb+Pb collisions, establishing a common multiplicity-dilution baseline for background-driven charge correlations. In contrast, Ru+Ru, Zr+Zr, and Au+Au collisions show significant deviations from this scaling trend. These violations are qualitatively similar to those obtained in AVFD calculations with an input chiral magnetic effect (CME) signal and point to an additional charge-separation component beyond that expected from the observed background scaling. Quantitative estimates indicate that, in mid-central collisions, the corresponding CME-sensitive fraction of the measured $\Delta\gamma/v_2$ is approximately 27% for Au+Au collisions and roughly a factor of two smaller for Ru+Ru and Zr+Zr collisions, which exhibit similar magnitudes within uncertainties. The extracted magnitudes imply an expected Ru+Ru–Zr+Zr signal difference of only ∼1.3%, suggesting limited sensitivity of the Δγ correlator to the small difference expected between the isobar signals.

25.75.-q, 25.75.Gz, 25.75.Ld

In relativistic ion-ion collisions, metastable domains of gluon fields with non-trivial topological configurations [1,2] can form in the magnetized chiral quark-gluon plasma (QGP) [3–7]. The incoming ions generate a strong magnetic field, B, at early times [8,9]. The interaction of chiral quarks with topological gluon fields can produce an imbalance between left- and right-handed quarks, leading to an electric current $J_V=(N_c\, eB/2\pi^2)\mu_A$ along the magnetic-field direction. Here, N_c is the color factor, and μ_A is the axial chemical potential that quantifies the axial charge imbalance [10–13]. The resulting final-state charge separation, known as the chiral magnetic effect (CME) [3], is of considerable interest, but its experimental characterization is complicated by large charge-dependent background correlations.

The charge separation can be quantified through the first P-odd sine coefficient, a_1, in the Fourier decomposition of the charged-particle azimuthal distribution [14],

$$\frac{dN_{ch}}{d\phi} \propto 1 + 2\sum_n [v_n \cos(n\Delta\phi) + a_n \sin(n\Delta\phi) + \cdots] \quad (1)$$

where $\Delta\varphi=\varphi-\Psi_{RP}$ is the particle azimuthal angle relative to the reaction-plane angle Ψ_{RP}, and v_n and a_n denote the P-even and P-odd Fourier coefficients, respectively. A direct measurement of a_1 is not possible because of the global P and CP symmetry of QCD. However, its fluctuations, characterized by $\tilde{a}_1=\langle a_1^2\rangle^{1/2}$, can be accessed via charge-sensitive observables, most notably the γ correlator [14].

The γ correlator is defined as

$$\gamma_{\alpha\beta} = \langle \cos(\phi_\alpha + \phi_\beta - 2\Psi_2) \rangle, \qquad \Delta\gamma = \gamma_{OS} - \gamma_{SS} \tag{2}$$

where Ψ_2 denotes the second-order event-plane angle, φ denotes the particle azimuthal emission angle, α,β denote the electric charge (+) or (-), and OS and SS represent opposite-sign and same-sign charge pairs, respectively. Equivalently, the three-particle correlation method [14–16] evaluates the correlator as

$$\gamma_{\alpha\beta} = \frac{\langle \cos(\phi_\alpha + \phi_\beta - 2\phi_\kappa) \rangle}{v_{2,\kappa}}, \qquad \Delta\gamma = \gamma_{OS} - \gamma_{SS} \tag{3}$$

where φ_κ is the azimuthal angle of a third particle κ used to estimate Ψ_2, and $v_{2,\kappa}$ is the corresponding elliptic-flow resolution factor.

Experimental measurements indicate significant Δγ in p+Au, d+Au, Ru+Ru, Zr+Zr, and Au+Au collisions at RHIC [15–21], and in p+Pb and Pb+Pb collisions at the LHC [22–26]. However, in addition to a possible CME-driven signal, the measured Δγ contains substantial charge-dependent background correlations arising from sources such as local charge conservation, resonance decays, and other non-flow effects [14,27–31]. Because many background sources involve correlations among a finite subset of particles embedded within a much larger event, their contribution to $\Delta\gamma/v_2$ is expected to undergo multiplicity dilution and exhibit a near-$1/N_{ch}$ scaling behavior that is largely insensitive to the specific microscopic origin of the correlations. A generalized empirical form for quantifying possible departures from this baseline scaling is

$$\frac{\Delta\gamma}{v_2} = a + \frac{b}{N_{ch}^{1-c}} \tag{4}$$

where a is an effective offset, b sets the magnitude of the multiplicity-dependent contribution, and c characterizes the degree of scaling violation. For background-dominated charge separation, $c\approx 0$ recovers the expected near-$1/N_{ch}$ scaling of $\Delta\gamma/v_2$. Positive values of c indicate deviations from this background scaling and point to an additional charge-separation component beyond that expected from multiplicity dilution alone.

The AVFD model [32,33] is used to provide a benchmark for the scaling patterns expected for background and signal+background contributions to $\Delta\gamma/v_2$ in A+A collisions. The resulting scaling patterns are then compared with those from previously published measurements for p+Au, d+Au, Ru+Ru, Zr+Zr, and Au+Au collisions at RHIC [15–21], together with p+Pb and Pb+Pb collisions at the LHC [22–25]. The CME signal is expected to be strongly suppressed in p(d)+A collisions because the magnetic field is significantly reduced and the event plane is only weakly correlated with the impact parameter and the magnetic-field direction [34–36]. At the same time, these systems contain substantial charge-dependent background correlations. Accordingly, the observed scaling properties of $\Delta\gamma/v_2$ in p(d)+A collisions provide an important experimental benchmark for validating the expected multiplicity-dilution scaling of background-driven charge correlations. Comparisons with larger collision systems then allow this scaling baseline to be tested across markedly different collision geometries and particle-production environments.

The AVFD model provides an essential benchmark for assessing the expected scaling behavior of the background and signal+background contributions to $\Delta\gamma/v_2$. The model simulates charge separation arising from the combined effects of the CME and charge-dependent backgrounds [33,32]. In brief, the event-by-event version of AVFD employs Monte Carlo Glauber initial conditions to simulate the evolution of fermion currents in the QGP, coupled to the bulk medium evolution implemented with the VISHNU hydrodynamic framework [37], followed by a hadronic transport stage modeled with URQMD. Background-driven charge-dependent correlations arise primarily from local charge conservation (LCC) on the freeze-out hypersurface and resonance decays. The CME signal is generated through the combined action of a time-dependent magnetic field, $B(\tau)=B_0/[1+(\tau/\tau_B)^2]$, and a nonzero initial axial charge density n_5/s, which induces an electric current along the magnetic-field direction. The peak magnetic-field values B_0 are obtained from event-by-event simulations [38], and a relatively conservative lifetime τ_B=0.6 fm/c is employed. The initial axial charge density, arising from topological gluonic fluctuations in the early-time glasma, together with the LCC fraction, controls the relative magnitudes of the CME signal and the background correlations.

Simulated AVFD events were generated for a broad range of centralities and input values of n_5/s and LCC fraction to establish the expected scaling patterns for background-only and signal+background contributions to $\Delta\gamma/v_2$, and to quantify the scaling violations expected when a CME component is present. Together with the experimentally observed scaling in background-dominated collision systems, these calculations provide a benchmark for interpreting the scaling properties of the experimental measurements.

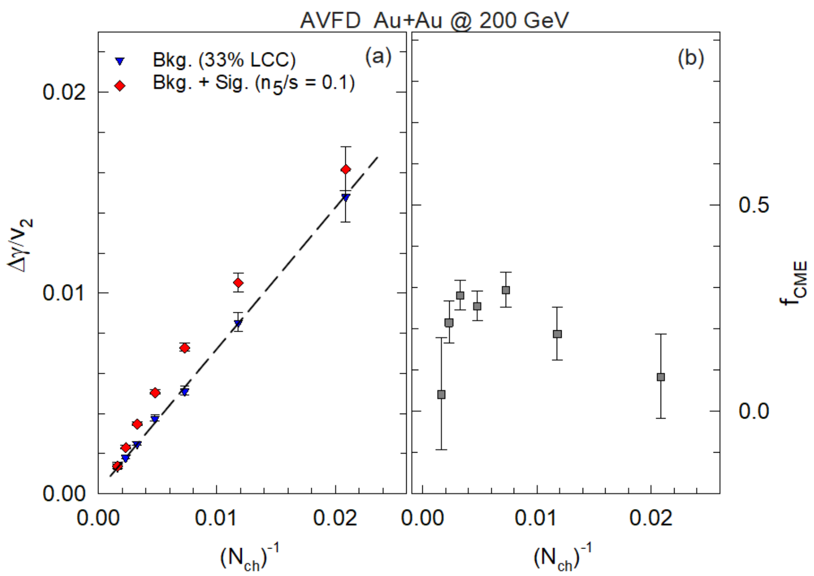

<u>FIG. 1</u>: $\Delta\gamma/v_2$ versus $1/N_{ch}$ (a) and f_{CME} versus $1/N_{ch}$ (b) for simulated Au+Au collisions at $\sqrt{s_{NN}}$ = 200 GeV obtained with the AVFD model. The $\Delta\gamma/v_2$ results are shown separately for the background and signal+background contributions as indicated. The dashed line

in (a) is a linear fit to the background values and illustrates the expected $1/N_{ch}$ scaling associated with multiplicity dilution of charge-dependent background correlations. The f_{CME} values in (b), obtained from Eq. (5), quantify the CME-sensitive fraction of the total charge-separation signal in the model calculations.

The centrality dependence of the $\Delta\gamma/v_2$ values obtained from AVFD events is summarized for Au+Au collisions in Fig. 1. To highlight the scaling behavior of the background, $\Delta\gamma/v_2$ is plotted as a function of $1/N_{ch}$. The solid triangles in Fig. 1(a) show that the background contribution follows the expected $1/N_{ch}$ dependence associated with the multiplicity dilution of charge-dependent non-flow correlations, corresponding to the limiting case $c \approx 0$ in Eq. (4). By contrast, the signal+background results exhibit positive deviations from this scaling behavior, consistent with the scaling violations characterized by $c>0$. In the AVFD framework, these deviations arise from the input CME signal and therefore provide a benchmark for assessing how CME-driven charge separation manifests as a violation of the background-scaling baseline. The magnitude of the CME-sensitive component can be quantified through the fraction

$$f_{\mathrm{CME}} = \frac{[\Delta\gamma/v_2(\mathrm{Sig.}+\mathrm{Bkg.}) - \Delta\gamma/v_2(\mathrm{Bkg.})]}{[\Delta\gamma/v_2(\mathrm{Sig.}+\mathrm{Bkg.})]} \tag{5}$$

which is shown as a function of $1/N_{ch}$ in Fig. 1(b). The figure indicates $f_{CME} \approx 30\%$ for 30–40% central Au+Au collisions, providing a useful benchmark for the sensitivity of the $\Delta\gamma$ correlator to CME-driven charge separation with input parameters $n_5/s=0.1$ and LCC=33%. Figure 1(b) also shows that the f_{CME} values peak in mid-central collisions but approach zero for both large and small N_{ch}, corresponding to central and peripheral collisions, respectively. This behavior indicates comparable background and signal+background values of $\Delta\gamma/v_2$ in these regions and motivates the use of the central and peripheral measurements as anchors for constraining the background contribution over the full centrality range.

The scaling patterns in Fig. 1(a) suggest that the observation of approximate $1/N_{ch}$ scaling in experimental $\Delta\gamma/v_2$ measurements would provide strong evidence that the measured charge separation is dominated by background-driven correlations. Conversely, significant deviations from this scaling could indicate an additional charge-separation component beyond that expected from multiplicity dilution alone. In the AVFD framework, such deviations arise from the input CME signal and therefore serve as a benchmark for assessing the scaling method's sensitivity to CME-driven charge separation.

Figure 1(b) also shows that the inferred f_{CME} values become small in both central and peripheral collisions, indicating comparable background and signal+background values of $\Delta\gamma/v_2$ in these regions. This behavior is consistent with the expected reduction of the magnetic field in central collisions and the substantial decorrelation between the event plane and the magnetic-field direction in peripheral collisions. Consequently, the $\Delta\gamma/v_2$ measurements in the central and peripheral regions provide natural anchors for constraining the background contribution through the observed $1/N_{ch}$ scaling. If residual CME-sensitive contributions remain in these anchoring regions, they would tend to increase the inferred background level and therefore render the extracted excess component conservative.

The v_2 and Δγ values reported for p+Au, d+Au, Ru+Ru, Zr+Zr, and Au+Au collisions at RHIC [15–17,19–21], together with p+Pb and Pb+Pb collisions at the LHC [23–26], were used to investigate the scaling properties of $\Delta\gamma/v_2$. Figure 2 shows the results for p+Pb and Pb+Pb collisions at $\sqrt{s_{NN}}$=5.02 TeV. The measurements exhibit a common approximate $1/N_{ch}$ scaling behavior over a broad multiplicity range, consistent with the expected multiplicity dilution of background-driven charge correlations. The p+Pb results provide an important validation benchmark because CME-driven charge separation is expected to be strongly suppressed in these collisions. The observed scaling therefore indicates that the substantial and multifaceted charge-dependent backgrounds present in p+Pb collisions follow the expected multiplicity-dilution behavior and do not generate significant violations of the $1/N_{ch}$ scaling.

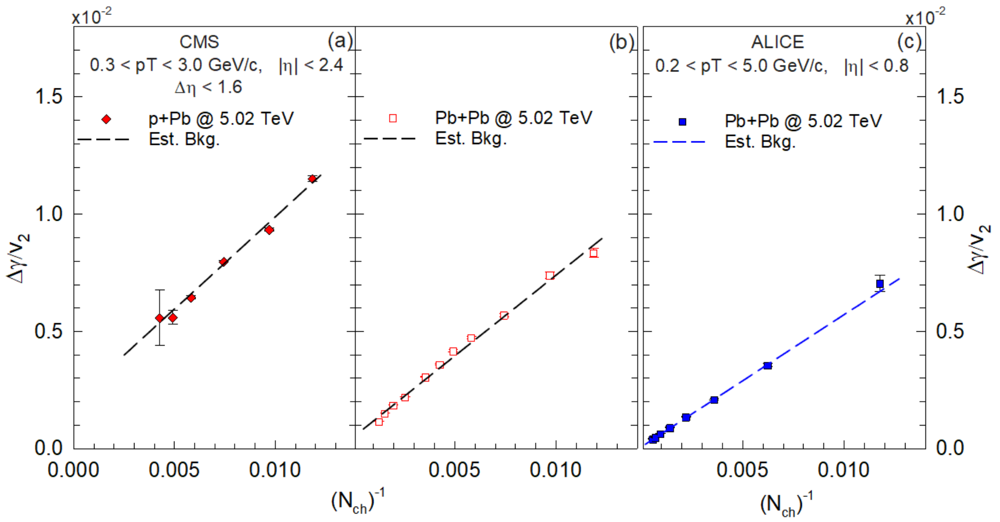

FIG. 2: $\Delta\gamma/v_2$ versus $1/N_{ch}$ for p+Pb (a) and Pb+Pb [(b) and (c)] collisions at $\sqrt{s_{NN}}$ = 5.02 TeV. The dashed lines indicate the expected $1/N_{ch}$ scaling behavior associated with multiplicity dilution of charge-dependent background correlations and provide an estimate of the background contribution. The observed scaling behavior in both p+Pb and Pb+Pb collisions indicates no significant scaling violation over the measured multiplicity range. The data are taken from Refs. [24-26].

The observation of the same scaling behavior in Pb+Pb collisions, despite their markedly different geometry and particle-production environment, suggests that any CME-sensitive contribution to the measured charge separation is small compared to the dominant background-driven correlations. A similar conclusion is supported by the results shown in Fig. 3 for Pb+Pb collisions at $\sqrt{s_{NN}}$=2.76 TeV. These measurements were obtained with event-shape selection based on fractional cuts of the magnitude of the q_2 flow-vector distribution [39], thereby selecting event classes with substantially different elliptic-flow magnitudes that reflect differences in the underlying initial geometry. The corresponding q_2 selections are indicated in the figure. Despite these variations, the measurements remain consistent with the same approximate $1/N_{ch}$ scaling behavior established by the p+Pb measurements, providing additional support for the robustness and universality of the multiplicity-dilution scaling expected for background-driven charge correlations.

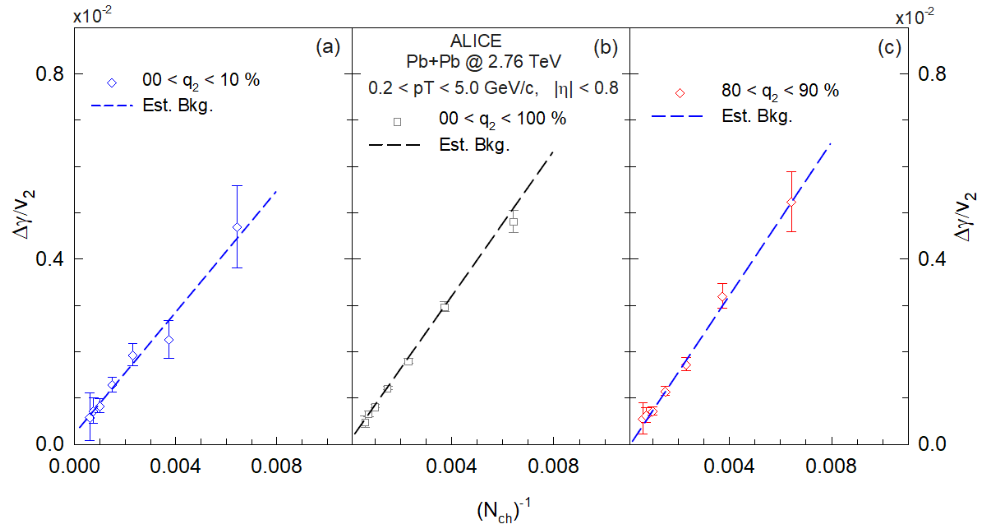

<u>FIG. 3</u>: $\Delta\gamma/v_2$ versus $1/N_{ch}$ for q_2-selected Pb+Pb collisions at $\sqrt{s_{NN}}$ = 2.76 TeV. The dashed lines indicate the expected $1/N_{ch}$ scaling behavior associated with multiplicity dilution of charge-dependent background correlations and provide an estimate of the background contribution. The measurements remain consistent with the observed scaling trend across the different event-shape selections. The data are taken from Ref. [23].

The scaling results for RHIC collisions at $\sqrt{s_{NN}}$=200 GeV are shown in Figs. 4 and 5. The results for d+Au collisions exhibit the same approximate $1/N_{ch}$ scaling observed for p+Pb collisions [cf. Fig. 2(a)], consistent with the expectation that CME-driven charge separation is strongly suppressed in p(d)+A collisions. Similar scaling behavior is observed for p+Au collisions (not shown), albeit with larger statistical uncertainties. Together with the p+Pb and Pb+Pb results, these measurements establish a common multiplicity-dilution scaling baseline for background-driven charge separation. In contrast, the measurements for Au+Au [Fig. 4(b)], Ru+Ru [Fig. 5(a)], and Zr+Zr [Fig. 5(c)] exhibit visible deviations from this common $1/N_{ch}$ scaling trend. The observed scaling violations are qualitatively similar to those obtained for the signal+background AVFD calculations shown in Fig. 1(a), indicating the presence of an additional charge-separation component beyond that expected from the observed background scaling.

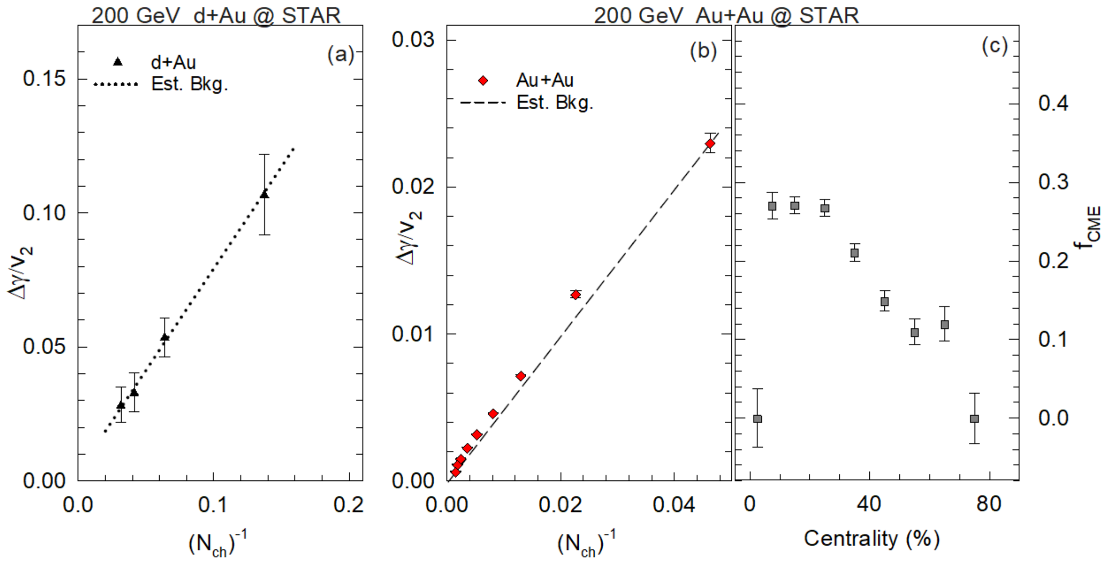

FIG. 4: $\Delta\gamma/v_2$ versus $1/N_{ch}$ [(a) and (b)] and the extracted f_{CME} versus centrality (c) for d+Au and Au+Au collisions at $\sqrt{s_{NN}}$ = 200 GeV. Panel (a) provides an experimental benchmark for the expected background scaling. The dotted and dashed lines indicate the expected $1/N_{ch}$ scaling behavior associated with multiplicity dilution of charge-dependent background correlations and provide estimates of the background contribution. The f_{CME} values shown in panel (c), obtained from Eq. (5), quantify the extracted CME-sensitive fraction for Au+Au collisions as a function of centrality.

To quantify the magnitude of this additional component, f_{CME} [Eq. (5)] is evaluated following an estimate of the background contribution to $\Delta\gamma/v_2$. As discussed previously, the background estimate is constrained by the approximately $1/N_{ch}$ scaling observed in the central and peripheral measurements, with both the AVFD calculations and the data indicating minimal CME contributions. Together with the common multiplicity-dilution scaling established by the p(d)+A, p+Pb, and Pb+Pb measurements and supported by the AVFD calculations, these central and peripheral measurements provide anchor points for estimating the background contribution over the full centrality range; see Figs. 1(a), 2(a), and 4(a). The resulting background estimates are indicated by the dashed lines in Figs. 4(b), 5(a), and 5(c). The extracted f_{CME} values are shown as a function of centrality in Figs. 4(c), 5(b), and 5(d) for Au+Au, Ru+Ru, and Zr+Zr collisions, respectively. They indicate a non-negligible CME-sensitive component that varies with centrality. For mid-central Au+Au collisions, f_{CME}≈27%, approximately a factor of two larger than the values obtained for Ru+Ru and Zr+Zr. Within the quoted uncertainties, no significant difference is observed between the f_{CME} values for Ru+Ru and Zr+Zr, suggesting that the $\Delta\gamma$ correlator is sensitive to CME-driven charge separation in isobaric systems but may lack sufficient sensitivity to resolve the expected difference in their signal strengths [21]. An estimate based on the extracted f_{CME} magnitudes and the expected ~10% difference in CME signal strength between Ru+Ru and Zr+Zr collisions [21] indicates an observable difference of only ~1.3%, well below the current experimental uncertainties.

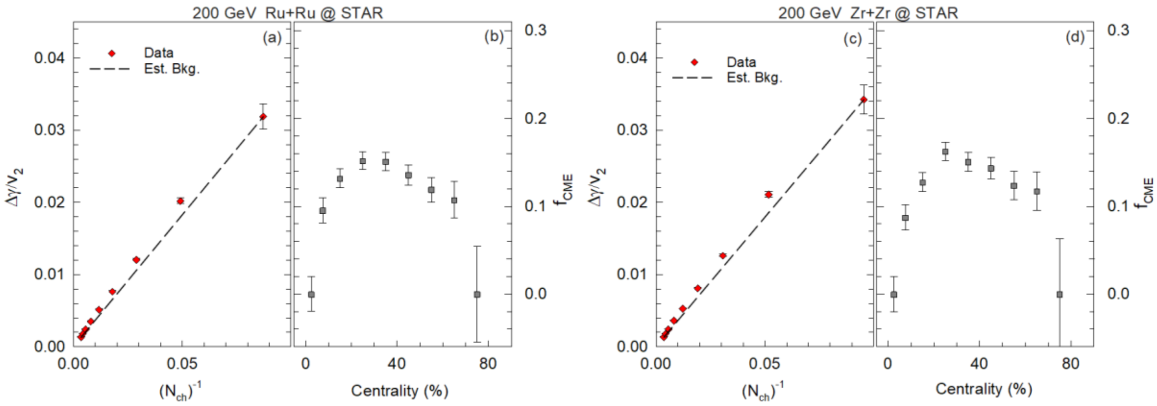

<u>FIG. 5</u>: $\Delta\gamma/v_2$ vs. $1/N_{ch}$ [(a) and (c)] and f_{CME} vs. centrality [(b) and (d)] for Ru+Ru and Zr+Zr collisions at $\sqrt{s_{NN}}$ = 200 GeV. The dashed lines indicate an estimate of the background contributions. The f_{CME} values in (b) and (d) characterize the fraction of the charge separation which is CME-driven (cf. Eq. 5). The data are taken from Ref. [21].

In summary, the scaling properties of the $\Delta\gamma$ correlator provide new constraints on the origin of charge separation across several collision systems at RHIC and the LHC. The ratio $\Delta\gamma/v_2$ for p+Au and d+Au collisions at $\sqrt{s_{NN}}$=200 GeV, together with p+Pb collisions at $\sqrt{s_{NN}}$=5.02 TeV and Pb+Pb collisions at $\sqrt{s_{NN}}$=5.02 and 2.76 TeV, exhibits a common approximate $1/N_{ch}$ scaling behavior consistent with the expected multiplicity dilution of background-driven charge correlations. These measurements establish a common scaling baseline for background-driven charge separation across collision systems with markedly different geometries, particle-production environments, and background compositions. In contrast, the measurements for Ru+Ru, Zr+Zr, and Au+Au collisions show significant deviations from this common scaling trend. The observed scaling violations are qualitatively similar to those obtained in AVFD calculations with an input CME signal and point to an additional charge-separation component beyond that expected from the observed background scaling. Quantitative estimates of this component indicate that the corresponding CME-sensitive fraction of the measured $\Delta\gamma/v_2$ signal is approximately 27% for mid-central Au+Au collisions and roughly a factor of two smaller for Ru+Ru and Zr+Zr collisions, which exhibit similar magnitudes within uncertainties. The extracted magnitudes imply an expected Ru+Ru–Zr+Zr signal difference of only ~1.3%, suggesting that, while the $\Delta\gamma$ correlator can detect a CME-related component in the isobar systems, it may lack sufficient sensitivity to resolve the small difference expected between their signal strengths.

*Email: Roy.Lacey@stonybrook.edu

Acknowledgments: This research is supported by the US Department of Energy, Office of Science, Office of Nuclear Physics, under contracts DE-SC0024602.

REFERENCES

[1] T. D. Lee, A Theory of Spontaneous T Violation, Phys. Rev. D 8, 1226–1239 (1973)

[2] Dmitri Kharzeev, R. D. Pisarski, and Michel H. G. Tytgat, Possibility of spontaneous parity violation in hot QCD, Phys. Rev. Lett. 81, 512–515 (1998), arXiv:hep-ph/9804221

[3] Dmitri Kharzeev, Parity violation in hot QCD: Why it can happen, and how to look for it, Phys. Lett. B633, 260–264 (2006), arXiv:hep-ph/0406125

[4] Jinfeng Liao, Anomalous transport effects and possible environmental symmetry 'violation' in heavy-ion collisions, Pramana 84, 901–926 (2015), arXiv:1401.2500 [hep-ph]

[5] Vladimir A. Miransky and Igor A. Shovkovy, Quantum field theory in a magnetic field: From quantum chromodynamics to graphene and Dirac semimetals, Phys. Rept. 576, 1–209 (2015), arXiv:1503.00732 [hep-ph]

[6] Xu-Guang Huang, Electromagnetic fields and anomalous transports in heavy-ion collisions -- A pedagogical review, Rept. Prog. Phys. 79, 076302 (2016), arXiv:1509.04073 [nucl-th]

[7] D. E. Kharzeev, J. Liao, S. A. Voloshin, and G. Wang, Chiral magnetic and vortical effects in high-energy nuclear collisions—A status report, Prog. Part. Nucl. Phys. 88, 1–28 (2016), arXiv:1511.04050 [hep-ph]

[8] Dmitri E. Kharzeev, Larry D. McLerran, and Harmen J. Warringa, The Effects of topological charge change in heavy ion collisions: 'Event by event P and CP violation', Nucl. Phys. A 803, 227–253 (2008), arXiv:0711.0950 [hep-ph]

[9] Masayuki Asakawa, Abhijit Majumder, and Berndt Muller, Electric Charge Separation in Strong Transient Magnetic Fields, Phys. Rev. C 81, 064912 (2010), arXiv:1003.2436 [hep-ph]

[10] Kenji Fukushima, Dmitri E. Kharzeev, and Harmen J. Warringa, The Chiral Magnetic Effect, Phys. Rev. D78, 074033 (2008), arXiv:0808.3382 [hep-ph]

[11] Dam T. Son and Piotr Surowka, Hydrodynamics with Triangle Anomalies, Phys. Rev. Lett. 103, 191601 (2009), arXiv:0906.5044 [hep-th]

[12] Valentin I. Zakharov, Chiral Magnetic Effect in Hydrodynamic Approximation, (2012), 10.1007/978-3-642-37305-3-11, [Lect. Notes Phys.871,295(2013)], arXiv:1210.2186 [hep-ph]

[13] Kenji Fukushima, Views of the Chiral Magnetic Effect, Lect. Notes Phys. 871, 241–259 (2013), arXiv:1209.5064 [hep-ph]

[14] Sergei A. Voloshin, Parity violation in hot QCD: How to detect it, Phys. Rev. C70, 057901 (2004), arXiv:hep-ph/0406311 [hep-ph]

[15] B. I. Abelev et al. (STAR), Observation of charge-dependent azimuthal correlations and possible local strong parity violation in heavy ion collisions, Phys. Rev. C 81, 054908 (2010), arXiv:0909.1717 [nucl-ex]

[16] B. I. Abelev et al. (STAR), Azimuthal Charged-Particle Correlations and Possible Local Strong Parity Violation, Phys. Rev. Lett. 103, 251601 (2009), arXiv:0909.1739 [nucl-ex]

[17] L. Adamczyk et al. (STAR), Fluctuations of charge separation perpendicular to the event plane and local parity violation in $\sqrt{s_{NN}}$ = 200 GeV Au+Au collisions at the BNL Relativistic Heavy Ion Collider, Phys. Rev. C88, 064911 (2013a), arXiv:1302.3802 [nucl-ex]

[18] L. Adamczyk et al. (STAR), Fluctuations of charge separation perpendicular to the event plane and local parity violation in $\sqrt{s_{NN}}$ = 200 GeV Au+Au collisions at the BNL Relativistic Heavy Ion Collider, Phys. Rev. C 88, 064911 (2013b), arXiv:1302.3802 [nucl-ex]

[19] L. Adamczyk et al. (STAR), Beam-energy dependence of charge separation along the magnetic field in Au+Au collisions at RHIC, Phys. Rev. Lett. 113, 052302 (2014a), arXiv:1404.1433 [nucl-ex]

[20] J. Adam et al. (STAR), Charge-dependent pair correlations relative to a third particle in p+Au and d+Au collisions at RHIC, Phys. Lett. B 798, 134975 (2019), arXiv:1906.03373 [nucl-ex]

[21] Mohamed Abdallah et al. (STAR), Search for the chiral magnetic effect with isobar collisions at $\sqrt{s_{NN}}$=200 GeV by the STAR Collaboration at the BNL Relativistic Heavy Ion Collider, Phys. Rev. C 105, 014901 (2022), arXiv:2109.00131 [nucl-ex]

[22] Betty Abelev et al. (ALICE), Charge separation relative to the reaction plane in Pb+Pb collisions at $\sqrt{s_{NN}}$ = 2.76 TeV, Phys. Rev. Lett. 110, 012301 (2013), arXiv:1207.0900 [nucl-ex]

[23] Shreyasi Acharya et al. (ALICE), Constraining the magnitude of the Chiral Magnetic Effect with Event Shape Engineering in Pb+Pb collisions at $\sqrt{s_{NN}}$ = 2.76 TeV, Phys. Lett. B 777, 151–162 (2018), arXiv:1709.04723 [nucl-ex]

[24] Vardan Khachatryan et al. (CMS), Observation of charge-dependent azimuthal correlations in p+Pb collisions and its implication for the search for the chiral magnetic effect, Phys. Rev. Lett. 118, 122301 (2017), arXiv:1610.00263 [nucl-ex]

[25] Albert M Sirunyan et al. (CMS), Constraints on the chiral magnetic effect using charge-dependent azimuthal correlations in p+Pb and Pb+Pb collisions at the CERN Large Hadron Collider, Phys. Rev. C 97, 044912 (2018), arXiv:1708.01602 [nucl-ex]

[26] Shreyasi Acharya et al. (ALICE), Constraining the Chiral Magnetic Effect with charge-dependent azimuthal correlations in Pb+Pb collisions at $\sqrt{s_{NN}}$ = 2.76 and 5.02 TeV, JHEP 09, 160 (2020), arXiv:2005.14640 [nucl-ex]

[27] Fuqiang Wang, Effects of Cluster Particle Correlations on Local Parity Violation Observables, Phys. Rev. C 81, 064902 (2010), arXiv:0911.1482 [nucl-ex]

[28] Adam Bzdak, Volker Koch, and Jinfeng Liao, Remarks on possible local parity violation in heavy ion collisions, Phys. Rev. C 81, 031901 (2010), arXiv:0912.5050 [nucl-th]

[29] Soren Schlichting and Scott Pratt, Charge conservation at energies available at the BNL Relativistic Heavy Ion Collider and contributions to local parity violation observables, Phys. Rev. C 83, 014913 (2011), arXiv:1009.4283 [nucl-th]

[30] L. Adamczyk et al. (STAR), Measurement of charge multiplicity asymmetry correlations in high-energy nucleus-nucleus collisions at $\sqrt{s_{NN}}$ = 200 GeV, Phys. Rev. C 89, 044908 (2014b), arXiv:1303.0901 [nucl-ex]

[31] Fuqiang Wang and Jie Zhao, Challenges in flow background removal in search for the chiral magnetic effect, Phys. Rev. C 95, 051901 (2017), arXiv:1608.06610 [nucl-th]

[32] Shuzhe Shi, Yin Jiang, Elias Lilleskov, and Jinfeng Liao, Anomalous Chiral Transport in Heavy Ion Collisions from Anomalous-Viscous Fluid Dynamics, Annals Phys. 394, 50–72 (2018), arXiv:1711.02496 [nucl-th]

[33] Yin Jiang, Shuzhe Shi, Yi Yin, and Jinfeng Liao, Quantifying the chiral magnetic effect from anomalous-viscous fluid dynamics, Chin. Phys. C 42, 011001 (2018), arXiv:1611.04586 [nucl-th]

[34] Vardan Khachatryan et al. (CMS), Observation of charge-dependent azimuthal correlations in p+Pb collisions and its implication for the search for the chiral magnetic effect, Submitted to: Phys. Rev. Lett (2016), arXiv:1610.00263 [nucl-ex]

[35] R. Belmont and J. L. Nagle, To CME or not to CME? Implications of p+Pb measurements of the chiral magnetic effect in heavy ion collisions, Phys. Rev. C96, 024901 (2017), arXiv:1610.07964 [nucl-th]

[36] Dmitri Kharzeev, Zhoudunming Tu, Aobo Zhang, and Wei Li, Effect of the fluctuating proton size on the study of the chiral magnetic effect in proton-nucleus collisions, Phys. Rev. C 97, 024905 (2018), arXiv:1712.02486 [nucl-th]

[37] Chun Shen, Zhi Qiu, Huichao Song, Jonah Bernhard, Steffen Bass, and Ulrich Heinz, The iEBE-VISHNU code package for relativistic heavy-ion collisions, Comput. Phys. Commun. 199, 61–85 (2016), arXiv:1409.8164 [nucl-th]

[38] John Bloczynski, Xu-Guang Huang, Xilin Zhang, and Jinfeng Liao, Azimuthally fluctuating magnetic field and its impacts on observables in heavy-ion collisions, Phys. Lett. B 718, 1529–1535 (2013), arXiv:1209.6594 [nucl-th]

[39] Jurgen Schukraft, Anthony Timmins, and Sergei A. Voloshin, Ultra-relativistic nuclear collisions: event shape engineering, Phys. Lett. B 719, 394–398 (2013), arXiv:1208.4563 [nucl-ex]